Applied Radiation and Isotopes 200 (2023) 110945

Contents lists available at ScienceDirect

Applied Radiation and Isotopes

journal homepage: www.elsevier.com/locate/apradiso

The international reference system for beta-particle emitting radionuclides: Validation through the pilot study CCRI(II)-P1.Co-60

Romain Coulon [a,*], Monica Aguiar Leobino da Silva [k], Emma Bendall [j], Denis E. Bergeron [d], Christophe Bobin [h], Ivana Bonková [c], Angus H.H. Bowan [n], Broda Ryszard [g], Marco Capogni [i], Mauro Capone [i], Pierluigi Carconi [i], Philippe Cassette [h], T. Cessna Jeffrey [d], Emily L. Clark [n], Sean Collins [j], Sammy Courte [a], Marek Czudek [g], Carlos José da Silva [k], Johnny de Almeida Rangel [k], Pierino De Felice [i], Fuyou Fan [l], Aldo Fazio [i], Ryan P. Fitzgerald [d], Carole Fréchou [h], Raphael Galea [f], Vincent Gressier [a], Akira Iwahara [k], Steven M. Judge [a], Christine M.B. Keevers [n], John Keightley [j], Karsten Kossert [b], Matej Krivošík [c], D.B. Kulkarni [e], Lizbeth Laureano-Perez [d], Edyta Lech [g], Anderson Leiras [k], Juncheng Liang [l], Paulo Alberto Lima da Cruz [k], Ronaldo Lins da Silva [k], Anna Listkowska [g], Haoran Liu [l], Meiling Liu [l], Joline Lubbe [m], Carine Michotte [a], Kimberly Moore [f], Ole Nähle [b], Manuel Nonis [a], Andy Pearce [j], Leticia Pibida [d], André L.L. Quadros [k], Natasha Ramirez [j], Anuradha Ravindra [e], Benoit Sabot [h], Paweł Saganowski [g], V. Sathian [e], Michael L. Smith [n], Ritu Sharma [e], Marcell P. Takács [b], Milton W. van Rooy [m], Robert Shearman [j], Martin J. van Staden [m], W.M. van Wyngaardt [n], Zhijie Yang [l], Melek Zarifi [n], Ming Zhang [l], Tomasz Ziemek [g]

[a] *Bureau International des Poids et Mesures, Pavillon de Breteuil, F-92312, Sèvres Cedex, France*
[b] *Physikalisch-Technische Bundesanstalt, Bundesallee 100, 38116, Braunschweig, Germany*
[c] *Slovenský Metrologický ústav, Karloveská 63, 842 55, Bratislava, Slovakia*
[d] *National Institute of Standards and Technology, 100 Bureau Drive, Gaithersburg, MD, 20899, USA*
[e] *Bhabha Atomic Research Centre, Mumbai, India*
[f] *National Research Council of Canada, 1200 Montreal Road, Ottawa, ON, K1A0R6, Canada*
[g] *National Centre for Nuclear Research Radioisotope Centre POLATOM, 05-400, Otwock, Poland*
[h] *Université Paris-Saclay, CEA, List, Laboratoire National Henri Becquerel (LNE-LNHB), F-91120, Palaiseau, France*
[i] *ENEA-Italian National Institute of Ionizing Radiation Metrology, Via Anguillarese - 301, I-00123, Roma, (IT), Italy*
[j] *National Physical Laboratory, Hampton Road Middlesex, TW11 0LW, Teddington, United Kingdom*
[k] *Laboratório Nacional de Metrologia das Radiações Ionizantes, Instituto de Radioproteção e Dosimetria, LNMRI/IRD, Av. Salvador Allende, 3773, CEP 22783-127, Barra da Tijuca, Rio de Janeiro, RJ, Brazil*
[l] *National Institute of Metrology (NIM), 100029, Beijing, China*
[m] *National Metrology Institute of South Africa, 15 Lower Hope Road, Rosebank, Cape Town, 7700, South Africa*
[n] *Australian Nuclear Science and Technology Organisation, Australia*

ARTICLE INFO

Keywords:
International system of reference
Standardization
Radionuclide metrology
Liquid scintillation counting
SIR
ESIR

ABSTRACT

The Bureau International des Poids et Mesures (BIPM) is developing a new transfer instrument to extend its centralized services for assessing the international equivalence of radioactive standards to new radionuclides. A liquid scintillation counter using the triple/double coincidence ratio method is being studied and tested in the CCRI(II)–P1.Co-60 pilot study. The pilot study, involving 13 participating laboratories with primary calibration capabilities, validated the approach against the original international reference system based on ionization chambers, which has been in operation since 1976. The results are in agreement and an accuracy suitable for purpose, below 5×10^{-4}, is achieved. The pilot study also reveals an issue when impurities emitting low-energy

* Corresponding author.
E-mail address: romain.coulon@bipm.org (R. Coulon).

https://doi.org/10.1016/j.apradiso.2023.110945
Received 25 May 2023; Received in revised form 14 June 2023; Accepted 13 July 2023
Available online 26 July 2023

electrons are present in the standard solution, which have a different impact on liquid scintillation counting compared to other primary measurement methods.

1. Introduction

The International Bureau of Weights and Measures (BIPM) operates the International Reference System (SIR), which provides international comparisons of radioactivity standardization capabilities. The way the SIR works provides the flexibility for National Metrology Institutes (NMIs) and Designated Institutes (DIs) to obtain a degree of equivalence for many gamma-ray-emitting radionuclides with a great deal of flexibility as to when it can be performed. Since 1976, the SIR response has served as the basis for precise and enduring Key Comparison Reference Values (KCRVs) for numerous radionuclides, including many with half-lives that preclude long-term comparisons with reference standards. From its inception until 31 December 2021, the SIR has been used to measure 1033 ampoules to give 788 independent results for 72 different radionuclides.

The system is based on a re-entrant ionization chamber and a specific approach to provide robust comparison values over decades (Karam et al., 2019; Ratel, 2007; Rytz, 1978). However, this system is not applicable to radionuclides that do not emit X- or γ-radiation during their decay. In addition, when only low-energy photons are emitted (for example ^{241}Am), the chamber response is significantly dependent on self-absorption by the source and ampoule. Recognizing this limitation, steps are being taken to expand the system's functionality to encompass radionuclides that do not emit X- or γ-radiation during their decay. This extension of the SIR, called the Extended SIR (ESIR), restarted its development in 2018 (Coulon et al., 2022a) with the implementation of a dedicated Liquid Scintillation (LS) counter and the so-called Triple-to-Double Coincidence Ratio (TDCR) standardization method (Broda, 2003). Liquid scintillation counting is adequate to detect ionizing α- or β-particles as well as very low energy x-rays emitted during electron capture decays directly since the radioactive material is embedded in the scintillator. The TDCR approach is used by the ESIR to correct, without using reference sources, for the slight changes that inevitably occur during long-term operation either in the detection efficiency or in the symmetry between the three photomultiplier tubes involved in the system. This feature has been demonstrated in preliminary studies simulating long-term instabilities via neutral density filters (Coulon et al., 2020a; Kossert et al., 2020).

Section II of the Consultative Committee for Ionizing Radiation (CCRI(II)) is responsible for supporting the International Committee for Weights and Measures (CIPM) in all matters concerning radionuclide metrology. Recognizing the value of the ESIR to the metrology community, the CCRI(II) decided to launch a pilot study CCRI(II)–P1.Co-60 to validate the ESIR against the SIR reference ionization chamber. Cobalt-60 has been selected due to its relatively high-energy β^- particles and γ-rays, which allow for easy measurement in both the SIR ionization chambers and the ESIR liquid scintillation counter. The pilot study involves conducting measurements on each submitted standard solution:

- with a measurement with the SIR ionization chamber (number 388),
- with a measurement with the ESIR liquid scintillation counter.

This pilot study was piloted by the BIPM and involved 13 participating laboratories listed in Table 1 with the date of BIPM measurements.

2. Materials and methods

Each participant was asked to prepare an SIR-type ampoule containing about 3.6 g of ^{60}Co standardized solution. A target activity concentration of about 100 kBq g^{-1} was requested from the participants in order to have a solution that is still measurable in the SIR ionization chamber and which allows the preparation of LS sources with acceptable radiation exposure. Participants were required to send their solution to the BIPM with a detailed measurement report including the activity per unit mass A_i, the reference date, an uncertainty budget showing the type A and B uncertainties, the list of detected impurities and their relative activity, the chemical form of the solution, its mass and its density. The

Table 1
Details of the participants in the CCRI(II)–P1.Co-60 pilot study, including the date of measurements at the BIPM.

Laboratory	Full name	Country	Measurement in the SIR	Measurement in the ESIR
PTB	Physikalisch-Technische Bundesanstalt	Germany	2020-07-30	2020-09-11
SMU	Slovensky Metrologicky Ustav	Slovakia	2020-11-04	2020-11-20
NIST	National Institute of Standards and Technology	United States	2020-11-09	2020-12-03
BARC	Bhabha Atomic Research Centre	India	2021-01-07	2021-01-14
NRC	National Research Council	Canada	2021-03-03	2021-03-16
POLATOM	National Centre for Nuclear Research Radioisotope Centre POLATOM	Poland	2021-03-03	2022-07-07
LNE-LNHB	Laboratoire National de métrologie et d'Essais -Laboratoire National Henri Becquerel	France	2021-03-04	2021-04-16
ENEA-INMRI	Agenzia nazionale per le nuove tecnologie, l'energia e lo sviluppo economico sostenibile - Istituto Nazionale di Metrologia delle Radiazioni Ionizzanti	Italy	2021-04-15	2021-05-08
NPL	National Physical Laboratory	United Kingdom	2021-05-03	2021-08-06
LNMRI-IRD	Laboratorio Nacional de Metrologia das Radiações Ionizantes	Brazil	2021-09-01	2021-10-22
NIM	National Institute of Metrology	China	2022-02-03	2022-02-17
NMISA	National Metrology Institute of South Africa	South Africa	2022-04-08	2022-07-06
ANSTO	Australian Nuclear Science and Technology Organisation	Australia	2022-08-29	2022-09-08

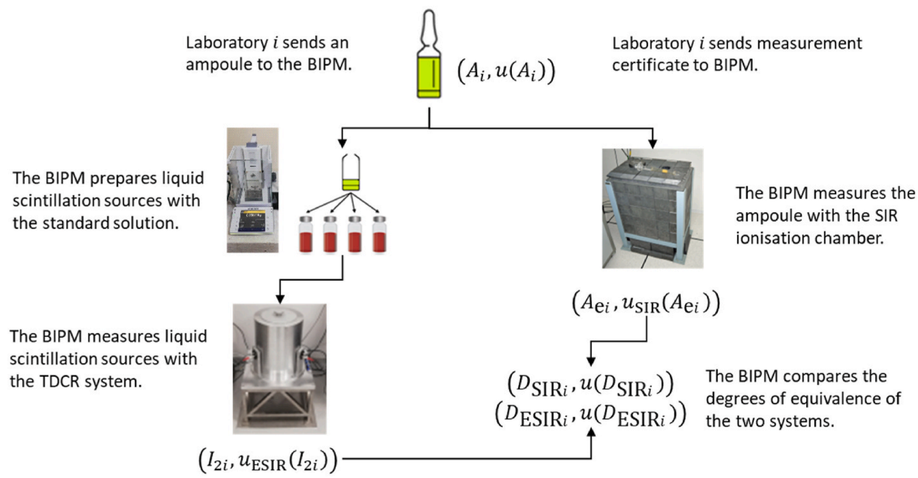

Fig. 1. Flowchart of the protocol of the pilot study.

protocol is summarized in Fig. 1.

After having received an ampoule, the BIPM measured the submitted ampoule using the SIR ionization chamber to obtain an equivalent activity A_{ei} with its associated standard uncertainty $u(A_{ei})$. At the request of the laboratory, and if the submission met all the eligibility requirements, the result was included in the official key comparison BIPM.RI(II)–K1.Co-60 (Coulon et al., 2023). Thereafter, the ampoule was opened, and several liquid scintillation sources were prepared using the differential weighing technique (Lourenço and Bobin, 2015) and a Mettler Toledo® balance with microgram accuracy.[1] For this study, glass vials and 10 mL of liquid scintillation cocktail were used. The measurement of these LS sources by the BIPM TDCR counter allowed the estimation of associated key comparison indicators, I_{0i}, I_{1i}, I_{2i} and related standard uncertainties $u(I_{0i})$, $u(I_{0i})$, $u(I_{0i})$, such as described in (Coulon et al., 2021). While

$$I_{0i} = \frac{R_{Di}}{m_i} \tag{1}$$

is only a simple indicator which corresponds to the ratio of the double coincidence count rates R_{Di} and the mass m_i of the aliquots of the radioactive solution put in the vial,

$$I_{1i} = \frac{I_{0i}(\alpha_1 + \alpha_2 + \alpha_3)}{\alpha_1 \left(\frac{R_{Ti}}{R_{Di}}\right)^2 + \alpha_2 \frac{R_{Ti}}{R_{Di}} + \alpha_3} \tag{2}$$

and

$$I_{2i} = \frac{I_{0i}}{\varepsilon\left(\frac{R_{Ti}}{R_{ABi}}, \frac{R_{Ti}}{R_{BCi}}, \frac{R_{Ti}}{R_{ACi}}, S, k_B, \frac{dE}{dx}\right)} \tag{3}$$

with R_{Ti} being the triple coincidence channel and R_{ABi}, R_{BCi}, R_{ACi} being the double coincidence count rates between two specific channels AB, BC and AC. I_{1i} and I_{2i} make use of the TDCR values to make the system more robust against efficiency/asymmetry changes in the TDCR system. I_{1i} implements a polynomial function of the global TDCR value R_{Ti}/R_{Di} with polynomial parameters $(\alpha_1, \alpha_2, \alpha_3)$. I_{1i} was slightly modified from its first introduction in (Coulon et al., 2020a, 2021) by adding the parameter α_3 in the polynomial function to achieve a gain in robustness when fitting the experimental curve from the efficiency changing procedure. Even though it was not critical for the ESIR final results, the weighing of the indicator by $(\alpha_1 + \alpha_2 + \alpha_3)$ makes an extrapolation to $TDCR = 1$, providing values with the same meaning as for the second indicator I_{2i}. In I_{2i}, a detection efficiency ε is calculated based on a statistical/physical model using the TDCR values, R_{Ti}/R_{ABi}, R_{Ti}/R_{BCi} and R_{Ti}/R_{ACi}, parametrized by the energy spectrum S, the Birks constant k_B, and the stopping power $\frac{dE}{dx}$. I_{1i} and I_{2i} can be seen as methods to estimate the activity of the solution. However, in the ESIR framework, it is important to note that the activity estimation is not the aim of these quantities called comparison indicators. The objective is to produce reference values that are robust against efficiency changing for I_{1i} or efficiency/asymmetry changing for I_{2i}. Therefore, the models will remain constant for a given radionuclide with fixed parameters $(\alpha_1, \alpha_2, \alpha_3)$ and $(S, k_B, \frac{dE}{dx})$ evaluated through a commissioning procedure described in (Coulon et al., 2020b) to maximize the robustness against efficiency variation. Although results using I_{0i} and I_{1i} will also be discussed, I_{2i} is considered as the reference parameter for the ESIR.

Finally, measurements from the SIR and the ESIR are used to produce degrees of equivalence

$$\delta_{SIR_i} = \frac{A_{ei} - KCRV_{SIR}}{KCRV_{SIR}} \tag{4}$$

and

$$\delta_{ESIR_i} = \frac{\kappa_i - KCRV_{ESIR}}{KCRV_{ESIR}}, \tag{5}$$

With $\kappa_i = \frac{A_i}{I_{2i}}$.

Relative degrees of equivalence are considered here in order to compare the ESIR with the SIR. The KCRV of the SIR considered in this pilot study is equal to 7062.0(23) kBq as published in the most recent comparison report (Coulon et al., 2023). In the context of this pilot study, the KCRV of the ESIR is defined by means of a link to the SIR using one laboratory result (NIST submission). This measure was taken because there were inconsistent values in this study. In official key comparisons, the uncertainty associated with the degrees of equivalence is expanded by a coverage factor $k = 2$ after combining the uncertainty from laboratories $u(A_i)$ with the uncertainty from the BIPM SIR measurement $u_{SIR}(A_{ei})$. However, to demonstrate the agreement between the two BIPM transfer instruments, only standard uncertainties are considered, taking into account only uncertainty components from the BIPM

[1] Certain commercial equipment, instruments, or materials are identified in this paper to foster understanding. Such identification does not imply recommendation by the participating national metrology institutes, nor does it imply that the materials or equipment identified are necessarily the best available for the purpose.

Table 2
Standardization methods and uncertainties of the participants.

Laboratory	Method	A_i /(kBq g^{-1})	T_0 (yy-mm-dd)	Relative standard uncertainty/10^{-2}		
				A	B	Comb.
ANSTO	4π(LS)β-γ anti-coincidence counting	86.97	2022-05-02	0.06	0.184	0.194
Source 1	Calibrated Ionization chamber[1]	85.20		0.035	0.234	0.237
ANSTO	4π(LS)β-γ coincidence counting	111.52	2022-05-02	0.058	0.123	0.136
Source 2	4π(LS)β-γ anti-coincidence counting	111.52		0.020	0.129	0.130
	4π(HPPC)β-γ coincidence counting[2]	111.54		0.035	0.171	0.175
BARC	4π(PC)β-γ coincidence counting[3]	78.30	2020-12-01	0.33	0.30	0.44
	4π(SP)β-γ coincidence counting[4]	78.34		0.48	0.42	0.64
	4π(LS)β-γ coincidence counting[5]	78.65		0.34	0.17	0.38
ENEA-INMRI	4π(NaI)γ integral counting	80.07	2021-02-16	0.30	0.27	0.41
	LS counting with TDCR method[6]	80.25		0.25	0.36	0.44
LNE-LNHB	4π(PC)β-γ anticoincidence counting	100.58	2021-02-22	0.10	0.10	0.14
	4π(LS)β-γ anticoincidence counting	100.48		0.19	0.10	0.21
	LS counting with TDCR method	100.57		0.10	0.22	0.24
LNMRI-IRD	4π(LS)β-γ anticoincidence counting	102.78	2020-08-20	0.30	0.10	0.32
	4π(LS)β-γ coincidence counting	101.82		0.64	0.06	0.64
	Ge(HP) γ rays peak-sum counting	102.79		0.08	0.21	0.22
	LS counting with TDCR method	102.24		0.26	0.11	0.28
NIM	4π(PC)β-γ coincidence counting	196.71	2020-09-18	0.12	0.21	0.24
	4π(LS)β-γ coincidence counting	196.51		0.17	0.24	0.29
NIST	4π(LS)β-γ anticoincidence counting	86.92	2020-10-01	0.19	0.12	0.22
NMISA	4π(LS)β-γ coincidence counting	225.56	2022-02-21	0.03	0.29	0.30
NPL	4π(LS)β-γ coincidence counting	98.32	2020-10-01	0.04	0.11	0.12
NRC	4π(PP)β-γ anticoincidence	104.10	2020-08-01	0.01	0.10	0.10
POLATOM	4π(LS)β-γ coincidence counting	598.64	2021-02-15	0.25	0.05	0.25
	4π(LS)β-γ anticoincidence counting	599.15		0.25	0.05	0.25
PTB	4π(PC)β-γ coincidence counting	101.029	2020-06-30	0.166	0.158	0.229
	4π(LS)β-γ coincidence counting	101.530		0.069	0.149	0.164
	LS counting with C/N method	101.510		0.050	0.221	0.227
	LS counting with TDCR method	101.530		0.042	0.174	0.180
SMU	LS counting with TDCR method	100.88	2020-09-15	0.22	0.30	0.37
	4π(LS)β-γ coincidence	101.16		0.45	0.28	0.53

[1] Calibrated by 4πβ-γ coincidence counting of source 2.
[2] Data was acquired using the ANSTO/NPL DCC system.
[3] Efficiency variation by source self-absorption.
[4] Efficiency variation was achieved by HV variation and optical filtering.
[5] Efficiency variation was achieved by chemical quenching.
[6] Using the Hidex 300 SL "Metro" version.

instruments $u_{\mathrm{SIR}}(A_{\mathrm{e}i})$ and $u_{\mathrm{ESIR}}(I_{2i})$ such that[2]

$$u(\delta_{\mathrm{SIR}i}) = \frac{\sqrt{KCRV_{\mathrm{SIR}}^2 u_{\mathrm{SIR}}^2(A_{\mathrm{e}i}) + A_{\mathrm{e}i}^2 u^2(KCRV_{\mathrm{SIR}})}}{KCRV_{\mathrm{SIR}}} \tag{6}$$

and

$$u(\delta_{\mathrm{ESIR}i}) = \frac{\sqrt{KCRV_{\mathrm{ESIR}}^2 u_{\mathrm{ESIR}}^2(\kappa_i) + \kappa_i^2 u^2(KCRV_{\mathrm{ESIR}})}}{KCRV_{\mathrm{ESIR}}}. \tag{7}$$

It should be noted that $\delta_{\mathrm{SIR}i}$ and $\delta_{\mathrm{ESIR}i}$ are not degrees of equivalence as they would be reported in key comparisons. They should not be used to assess consistency between laboratory standardization techniques but only to compare the results of the BIPM's two reference systems.

One additional measurement was realized at the LNE-LNHB using the μ-TDCR transportable system (Sabot et al., 2022) and based on the same LS sources measured at the LNE-LNHB for primary standardization. The analysis of the measurement files was done at the BIPM. This technology is being investigated as a possible transportable version of the ESIR.

The ANSTO has submitted two different solutions, one containing an impurity which emits beta particles (source 1), one free of impurities (source 2).

The NIM did not use SIR ampoules, which limits the relevance of the related SIR measurements in the pilot study.

3. Results

3.1. Activity measurements and standardization methods

A brief description of the standardization methods used by the participating laboratories is given in Table 2 with the relative standard uncertainties they claimed. More details are available in the corresponding BIPM.RI(II)–K1.Co-60 comparison reports (Coulon et al., 2023).

The two main measurement systems are proportional counters (5) and liquid scintillation counters (21). A variety of measurement methods are used, including 4πβ-γ coincidence counting (22), model-based approaches (five with TDCR and one with C/N), integral counting (one with an HPGe diode and one with a NaI(Tl) scintillator) and current measurement (one IC measurement by ANSTO). Gamma channels in 4πβ-γ coincidence counters are mainly based on NaI(Tl) scintillation detectors, except for PTB and NPL who equipped the LS systems with a $CeBr_3$ scintillation detector and a germanium detector, respectively. Six laboratories applied digital electronics in their setup:

- The NIM for 4πβ-γ coincidence counting based on PC and LS,

[2] Due to the large number of values (27) included in the KCRV calculation, possible correlations between $A_{\mathrm{e}i}$ and $KCRV_{\mathrm{SIR}}$ are not considered.

- LNMRI-IRD, PTB, NIST, and NPL for 4πβ-γ coincidence counting based on LS,
- ENEA-INMRI for integral counting,
- ANSTO for 4πβ-γ coincidence counting based on HPPC (NPL digital system).

The overall relative standard uncertainties associated with the activity measurement of the laboratories were in a range of 0.10%–0.64% with a median of 0.24%. This variety of systems and methods is an asset for the pilot study.

3.2. Nuclear decay data

The half-life used by the BIPM in the framework of the SIR[3] is 1925.5 (5) days as published in IAEA TECDOC-619 (IAEA, 1991). In the framework of the ESIR, the half-life used was 1925.23(29) days as published in the recommended *Monographie BIPM-5* (Bé et al., 2006). All the participants used this value, except for the PTB who used a half-life equal to 1925.3(4) days from a PTB report (PTB, 2000).

3.3. Standard solutions

The participating laboratories provided HCl solutions with a concentration of 0.1 mol dm^{-3}, except for ENEA-INMRI and NMISA, which reported concentrations of 1 mol dm^{-3} and 0.89 mol dm^{-3} respectively. The chemical carrier is $CoCl_2$ with various concentrations from 25 μg g^{-1} to 1000 μg g^{-1}. In accordance with the requirements of the SIR measurement, the laboratories provided about 3.6 g of solution with a density close to 1 g cm^{-3}.

Gamma-ray spectrometry of the solutions performed by many laboratories did not reveal the presence of photon-emitting impurities. However, the PTB reported three liquid scintillation-based measurements that were 0.5% higher than their proportional counter (PC) measurement. Their measurements were repeated with a solution submitted in 2001 and 2016 for which the results were found to be consistent. The PTB concluded that it is rather likely that the solution submitted in 2020 contains an impurity that cannot be identified by gamma-ray spectrometry. This impurity could be volatile when preparing solid sources for measurements in the proportional counter and/or could be low energetic and not be seen in a proportional counter or ionization chamber but seen in liquid scintillation counting. ANSTO observed an even higher discrepancy with their solution number 1 with LS based measurements 2.1% higher than their IC based measurement. The solution number 2 standardized by ANSTO shows a good agreement between PC and LS measurements, so it is assumed that it does not contain this type of impurity.

3.4. BIPM liquid scintillation sources

Table 3 presents the data associated with the preparation of liquid scintillation sources at the BIPM. Several LS sources were prepared from the standard solutions sent by laboratories for which is reported: the number N of LS sources produced, the average mass m_i of aliquots put in LS sources, the average pressure P, relative humidity H, and temperature T during the weighing procedure, the type of cocktail, and the average TDCR value measured by the TDCR system. Before preparing the LS sources, repeatability tests were carried out by weighing the pycnometer without droplet removal and at a frequency comparable to that of the preparation process. The measured mass differences are averaged to obtain an average drift specified for each preparation in the table.

The typical mass of solution deposited in LS vials was between 40 mg and 90 mg. The mass of solution was chosen so that the double coincidence count rates were between 5×10^3 s^{-1} and 1×10^4 s^{-1} except for POLATOM and NMISA for which N_D are equal to 2.5×10^4 s^{-1} and 1.4×10^4 s^{-1} respectively. No distilled water was added. The pycnometer filled with standard solution is weighed before and after droplet disposal in the vial using a Mettler Toledo XPE26C balance (re-calibrated each year by Mettler Toledo) and a U-shaped electrostatic remover. There is no air conditioning in the BIPM hot laboratory where sources are handled. The ambient conditions varied during the period of the pilot study with a temperature between 18 °C and 25 °C, a relative humidity varying from 33% to 61% and an atmospheric pressure in the range of 99.8 kPa–102.4 kPa. A buoyancy correction has been applied such as that recommended in (Lourenço and Bobin, 2015).

The average mass drift was always below ±5 μg leading to a relative impact on mass measurement contained below 2×10^{-4}.

Various types of LS cocktails were used. They are listed below:

- Cocktail "A": Ultima-Gold # SL CD-5360 used from September to December 2020
- Cocktail "B": Ultima-Gold # SL CF-4868 used from January to October 2021
- Cocktail "C": Ultima-Gold LLT from IRSN used from October 2021 to December 2022
- Cocktail "D": Ultima-Gold used by the LNE-LNHB for the μ-TDCR measurement.

The TDCR value is presented in Table 3 as an efficiency/quenching indicator for each batch of LS sources. The two batches of Ultima-Gold cocktails "A" and "B" provide equivalent measurements with TDCR values respectively equal to 0.9789(12) and 0.9785(4). The Ultima-Gold LLT batch "C" provides a slightly higher TDCR value equal to 0.9803(10) but still compatible with batches "A" and "B". Five sources were made with the LNMRI-IRD solution using the cocktail "B" and the other five using the cocktail "C". The set of measurements is consistent (chi-squared test) although different cocktails were used.

The consistency of the results between LS sources was checked using a chi-squared test while removing all correlated components in the uncertainty budget and keeping only the counting statistics uncertainty evaluated through 10 repeated measurements of 720 s. Comparison indicators I_1 and I_2 appears to be consistent for the different LS sources produced demonstrating the reliability of the weighing procedure. Two outliers have been detected, the NRC LS sources n° 2, and the PTB LS source n° 8, leading to an averaging among results from nine sources instead of the initial ten LS sources made for these laboratories.

3.5. The BIPM TDCR measurements

The Yantel nanoTDCR (Jordanov et al., 2020) was used for the TDCR measurement. Measurements are realized in four configurations:

- Configuration 1: an extended dead time of 50 μs and a coincidence resolving time of 50 ns,
- Configuration 2: an extended dead time of 50 μs and a coincidence resolving time of 100 ns,
- Configuration 3: an extended dead time of 10 μs and a coincidence resolving time of 50 ns,
- Configuration 4: an extended dead time of 10 μs and a coincidence resolving time of 100 ns.

Configuration 3, which minimizes both the extended dead time and the coincidence resolving time was chosen as the reference setup in this study. In this reference configuration, Table 4 shows the results from the TDCR system averaged among individual measurements of the LS sources. The double coincidence count rate, the measurement dead time and the accidental coincident rate (Dutsov et al., 2020) are presented.

[3] An update of the half-life involves recalculating all previously published equivalent activity values. This is only done when the update has a significant impact on the results.

Table 3
Characteristics of liquid scintillation sources produced by the BIPM with the number of LS sources (N), the average mass of aliquots (m_i), the pressure (P), the humidity (H), the temperature (T), the mean mass drift between consecutive weighings, the reference of the LS cocktail and the averaged TDCR parameter.

Laboratory	N	m_i /mg	P /kPa	H /10^{-2}	T /°C	Mean drift /µg	LS Cocktail	Averaged TDCR value
ANSTO (1)	5	74.44(80)	100.975(8)	52.6(6)	24.69(4)	2.4	C	0.980 6(2)
ANSTO (2)	5	70.0(13)	100.942(4)	52.0(4)	24.9(2)	−1.5	C	0.979 0(4)
BARC	10	60.4(33)	101.43(1)	38.2(5)	18.9(1)	0.6	B	0.978 6(9)
ENEA-INMRI	10	88.9(16)	100.48(3)	40.1(8)	20.57(7)	1.1	B	0.978 7(5)
LNE-LNHB	10	67.7(17)	102.38(2)	32.9(3)	20.85(3)	−0.7	B	0.978 6(4)
LNE-LNHB*	6	51.7(62)	99.4	39.4	22.4	NA	D	0.977 6(2)
LNMRI-IRD	10	59.0 (8)	101.28(1)	69.7(9)	20.57(9)	1.2	B/C	0.977 5(16)
NIM	10	39.9(8)	101.73(2)	47.1(4)	19.46(3)	4.7	C	0.981 1(5)
NIST	10	70.0(6)	101.78(2)	39.3(4)	18.34(5)	−1.0	A	0.977 8(7)
NMISA	5	51.47(21)	101.28(1)	45.0(3)	23.61(4)	−0.6	C	0.979 5(4)
NRC	9**	66.3(13)	99.80(3)	53.8(16)	20.37(1)	0.6	B	0.979 1(8)
NPL	10	77.8(11)	100.56(1)	61.2(2)	22.84(8)	2.0	B	0.977 9(3)
POLATOM	5	40.0(4)	101.22(1)	42.1(2)	24.02(7)	2.0	C	0.981 4(2)
PTB	9**	63.9(38)	101.83(2)	56.7(2)	22.66(7)	1.6	A	0.980 2(3)
SMU	10	63.7(15)	101.87(1)	55.6(2)	20.73(1)	−1.4	A	0.978 8(4)

*These LS sources were prepared at the LNE-LNHB.
**Outlier detected.

They show a good homogeneity in the counting configurations, with most of the count rates in a range from 6000 s^{-1}–7000 s^{-1}, inducing a measurement dead time contained below 10% and a relative accidental coincidence rate below 0.03%.

Furthermore, the comparison indicators are displayed showing that I_1 and I_2 are compatible within one standard deviation. The equivalence between these quantities demonstrates that the symmetry of the system was good during the comparison exercise.

The comparison indicators I_1 and I_2 required fixed parameters to be determined at first use of a radionuclide. For ^{60}Co, an efficiency changing procedure was applied using neutral density filters to determine parameters that provide to the system the best robustness against efficiency variation (see details in (Coulon et al., 2020b)). The polynomial parameters of I_1 are $\alpha_1 = 136080$, $\alpha_2 = -170474$, $\alpha_3 = 132853$. For the I_2 indicator, the energy spectrum $S(E)$ was estimated by Monte-Carlo simulation of the photon and electron transport using the PENELOPE code and decay data from the Co-60 PenNuc file available in the DDEP database. A Birks constant equal to 0.01 cm MeV^{-1} was used.

3.6. Final measurement results from the BIPM transfer instruments

Table 5 compiles the measurement results from the SIR. The standardization method and the activity A_i evaluated by the laboratories are presented. The equivalent activity A_{ei} is displayed with the standard uncertainty $u_{SIR}(A_{ei})$ from the SIR and the standard uncertainty $u_c(A_{ei})$ combining uncertainty contributions from the SIR and from the laboratory. More details are given in the last key comparison report (Coulon et al., 2023).

Table 6 contains the measurement results from the ESIR. The standardization method and the activity A_i evaluated by the laboratories are also stated. The comparison ratio $\kappa_i = A_i/I_{2,i}$ is displayed with the standard uncertainty $u_{ESIR}(\kappa_i)$ from the ESIR and the standard uncertainty $u_c(\kappa_i)$ combining uncertainty contributions from the ESIR and from the laboratory.

3.7. Comparison of degrees of equivalences

Using measurement results A_{ei} and κ_i from the SIR and ESIR, degrees of equivalence δ_{SIRi} and δ_{ESIRi} are calculated according to Eqs (4)–(7). The difference between the two DoE estimations, $\Delta_i = \delta_{ESIRi} - \delta_{SIRi}$, and associated standard deviations are calculated such that

$$u(\Delta_i) = \sqrt{u^2_{ESIR}(\delta_{SIRi}) + u^2_{SIR}(\delta_{ESIRi})}. \quad (8)$$

The figure of merit $Z = \frac{|\Delta_i|}{u(\Delta_i)}$, quantifies the agreement between the

Table 4
ESIR measurements in Configuration 3 with the double coincidence count rate, the measurement dead time, the false coincidence rate, and the comparison indicators I_{0i}, I_{1i} and I_{2i}.

Laboratory	Averaged double coincidence rate/s^{-1}	Averaged dead time /10^{-2}	Averaged False coincidence rate/10^{-4}	I_{0i} /(s^{-1} g^{-1})	I_{1i} /(Bq g^{-1})	I_{2i} /(Bq g^{-1})
ANSTO (1)	6185(66)	8.0(4)	1.0	84 771(18)	86 457(11)	86 489(10)
ANSTO (2)	7449(140)	9.9(8)	1.6	108 753(40)	111 098(33)	111 141(33)
BARC	4702(23)	8.0(7)	2.6	77 874(58)	79 578(22)	79 609(22)
ENEA-INMRI	6919(16)	9.9(9)	2.2	77 832(32)	79 529(14)	79 559(14)
LNE-LNHB	6635(20)	8.4(9)	1.9	98 005(32)	100 157(26)	100 196(26)
LNE-LNHB*[1]	5000(610)	10.8(10)	4.3	97 747(55)	99 994(51)	100 033(51)
LNMRI-IRD	5912(17)	7.0(2)	1.1	100 200(130)	102 514(42)	102 553(43)
NIM[2]	7688(19)	8.3(3)	1.1	192 670(82)	196 399(50)	196 468(50)
NIST	5928(8)	8.2(5)	1.5	84 683(58)	86 612(13)	86 645(13)
NMISA	13 729(56)	13.8(5)	1.9	220 311(59)	224 936(61)	225 021(62)
NPL	7530(110)	9.0(5)	1.4	95 798(18)	97 963(20)	98 001(20)
NRC	6730(130)	9.0(7)	1.9	101 498(62)	103 693(67)	103 712(57)
POLATOM	24 790(250)	22.9(7)	2.8	585 270(152)	596 437(200)	596 660(203)
PTB	6330(380)	8.9(6)	1.7	99 068(29)	101 076(15)	101 143(14)
SMU	6300(150)	8.4(2)	1.3	98 835(44)	100 985(42)	101 023(41)

[1]This additional measurement was done using the transportable µTDCR system at the LNE-LNHB (Sabot et al., 2022). The analysis of the measurement files was done at the BIPM. This technology is being investigated as a possible transportable version of the ESIR.
[2]Not in an SIR ampoule.

Table 5
Results from the SIR with the standardization method, the mass activity measurement by the laboratory (A_i), the equivalent activity measured by the SIR (A_{ei}), the relative standard uncertainty due to the SIR ($u_{SIR}(A_{ei})$) and the combined standard uncertainty ($u_c(A_{ei})$).

Laboratory	Method	Activity A_i /(Bq g^{-1})	A_{ei} /(kBq)	$u_{SIR}(A_{ei})$ /10^{-4}	$u_c(A_{ei})$
ANSTO (1)	LS anticoincidence	86 970(200)	7209	6	15
	Ionization chamber	85 200(200)	7062	6	18
ANSTO (2)	LS coincidence	111 520 (150)	7061	6	10
	LS anticoincidence	111 520 (150)	7061	6	11
	PC coincidence	111 540 (190)	7063	6	13
BARC	PC coincidence	78 300(340)	7037	6	32
	SP coincidence	78 340(500)	7041	6	46
	LS coincidence	78 650(300)	7069	6	28
ENEA-INMRI	Integral counting	80 070(330)	7096	7	30
	TDCR method	80 250(350)	7112	7	32
LNE-LNHB	PC anticoincidence	100 580 (140)	7070	8	12
	LS anticoincidence	100 480 (220)	7063	8	17
	TDCR method	100 570 (240)	7070	8	19
LNMRI-IRD	LS anticoincidence	102 784 (320)	7058	6	23
	LS coincidence	101 818 (650)	6991	6	45
	Peak-sum counting	102 791 (230)	7058	6	17
	TDCR method	102 240 (290)	7020	6	21
NIM	PC coincidence	196 710 (406)	7034	4	17
	LS coincidence	196 510 (570)	7027	4	21
NIST	LS anticoincidence	86 920(200)	7062	6	18
NMISA	LS coincidence	225 560 (670)	7068	4	21
NPL	LS coincidence	100 100 (100)	7058	6	10
NRC	PC anticoincidence	104 100 (100)	7068	9	11
POLATOM	LS coincidence	598 640 (1540)	7073	3	18
	LS anticoincidence	599 150 (1530)	7079	3	18
PTB	PC coincidence	101 029 (230)	7069	7	18
	LS coincidence	101 530 (170)	7104	7	14
	C/N method	101 510 (230)	7102	7	18
	TDCR method	101 530 (180)	7104	7	15
SMU	TDCR method	100 880 (380)	7047	6	27
	LS coincidence	101 160 (540)	7066	6	38

two measurement systems. According to a Z-test, the null hypothesis H_0: $\Delta_i = 0$ can be rejected with a risk of false rejection lower than 1% when $Z \geq 2.57$. The results are displayed in Table 7.

An agreement between the two systems is observed for the 20 measurements presented in Fig. 2.

The ESIR delivers significantly different results (see Fig. 3) than the SIR for eleven measurements from four laboratories: ANSTO, BARC, PTB and NIM.

In the case of the measurements made with the source 1 from ANSTO, large differences of about 19 standard deviations are observed

Table 6
Results from the ESIR with the standardization method, the mass activity measurement by the laboratory (A_i), the ESIR comparison ratio (κ_i), the relative standard uncertainty due to the ESIR ($u_{ESIR}(k_i)$) and the combined standard uncertainty ($u_c(k_i)$).

Laboratory	Method	Activity A_i /(Bq g^{-1})	$\kappa_i = A_i/I_{2,i}$	$u_{ESIR}(k_i)$	$u_c(k_i)$
ANSTO (1)	LS anticoincidence	86 970 (200)	1.005 65	0.000 12	0.002 32
	Ionization chamber	85 200 (200)	0.985 10	0.000 12	0.002 32
ANSTO (2)	LS coincidence	111 520 (150)	1.003 41	0.000 30	0.001 34
	LS anticoincidence	111 520 (150)	1.003 41	0.000 30	0.001 34
	PC coincidence	111 540 (190)	1.003 59	0.000 30	0.001 73
BARC	PC coincidence	78 300 (340)	0.983 56	0.000 27	0.004 28
	SP coincidence	78 340 (500)	0.984 06	0.000 27	0.006 29
	LS coincidence	78 650 (300)	0.987 95	0.000 27	0.003 78
ENEA-INMRI	Integral counting	80 070 (330)	1.006 42	0.000 18	0.004 15
	TDCR method	80 250 (350)	1.008 69	0.000 18	0.004 40
LNE-LNHB	PC anticoincidence	100 580 (140)	1.003 83 1.005 47*	0.000 26 0.000 51*	0.001 42 0.001 49*
	LS anticoincidence	100 480 (220)	1.002 83 1.004 47*	0.000 26 0.000 51*	0.002 21 0.002 26*
	TDCR method	100 570 (240)	1.003 73 1.005 37*	0.000 26 0.000 51*	0.002 41 0.002 45*
LNMRI-IRD	LS anticoincidence	102 784 (320)	1.002 25	0.000 42	0.003 15
	LS coincidence	101 818 (650)	0.992 83	0.000 42	0.006 35
	Peak-sum counting	102 791 (230)	1.002 32	0.000 42	0.002 28
	TDCR method	102 240 (290)	0.996 95	0.000 42	0.002 86
NIM	PC coincidence	196 710 (406)	1.001 23	0.000 26	0.002 91
	LS coincidence	196 510 (570)	1.000 21	0.000 26	0.002 41
NIST	LS anticoincidence	86 920 (200)	1.003 17	0.000 15	0.002 31
NMISA	LS coincidence	225 560 (670)	1.002 40	0.000 28	0.002 99
NPL	LS coincidence	100 100 (100)	1.012 78	0.000 22	0.001 03
NRC	PC anticoincidence	104 100 (100)	1.003 74	0.000 21	0.000 99
POLATOM	LS coincidence	598 640 (1540)	1.003 33	0.000 34	0.002 60
	LS anticoincidence	599 150 (1530)	1.004 18	0.000 34	0.002 59
PTB	PC coincidence	101 029 (230)	0.998 88	0.000 14	0.002 28
	LS coincidence	101 530 (170)	1.003 83	0.000 14	0.001 69
	C/N method	101 510 (230)	1.003 63	0.000 14	0.002 28
	TDCR method	101 530 (180)	1.003 83	0.000 14	0.001 79
SMU	TDCR method	100 880 (380)	0.998 58	0.000 41	0.003 78
	LS coincidence	101 160 (540)	1.001 36	0.000 41	0.005 36

(*)Using the measurements from the LNHB transportable instrument, the μ-TDCR.

between the SIR and the ESIR. This solution is known by ANSTO for containing pure beta impurities. The ionization chamber measurements at both the ANSTO and BIPM filters this type of impurity leading to $\delta_{\mathrm{SIR}i} \approx 0$ %. However, LS based measurement at both the ANSTO and BIPM do not necessarily filter this out hence $\delta_{\mathrm{SIR}i} \approx +2.1\%$. When the equivalence is evaluated by the ESIR, the opposite is observed with a large discrepancy $\delta_{\mathrm{ESIR}i} \approx -1.8$ % for the IC measurement. This shows that the interfering impurity affects the LS systems at the BIPM and ANSTO. On the basis of a spectrum analysis of these two solutions and an assessment of the mode of production of the radionuclide, ANSTO estimated that ^{14}C and ^{99}Tc could be contained in their solution (details are given in (van Wyngaardt, 2023)).

In the case of PTB measurements, an excellent agreement with the KCRV is obtained in the SIR framework for the PC measurement but a $\delta_{\mathrm{SIR}i} \approx +0.5$ % is observed for the three LS measurements. Again, there is a misleading opposite conclusion in the ESIR showing an agreement with the KCRV for the LS measurements made by PTB and a discrepant value for the PC measurement. Similar to the ANSTO case, it is noteworthy that the influence of this impurity in the two LS systems of PTB and BIPM is almost the same. The PTB used the same threshold (not filtering single electrons) for its 4π(LS)β-γ coincidence counting and its measurements based on free parameters (C/N and TDCR). As an equivalent threshold was implemented in the ESIR, this explains the similarity of the impact of impurities. It should be noted that PTB was aware of the problem of an impurity and the official final laboratory result is based solely on 4πβ(PC)-γ coincidence counting.

A significant relative deviation of about −1.5% is observed with ESIR evaluations for the BARC submission. This difference is the same regardless of whether the laboratory measurement is done via LS or PC. The laboratory did not report the presence of impurities and inferring on this presence is less straightforward than in the ANSTO and PTB cases. However, unlike the model-based LS techniques (TDCR or C/N), the impact of a low-energy emitting impurity could have been filtered with the BARC 4π(LS)β-γ coincidence system. The use of a single PMT in the beta channel allowed for the threshold to be set at a sufficiently high level to avoid thermionic noise, which in turn prevented the system from detecting any potential low-energy emitting impurities.

The NIM results also display a significant difference between the SIR and the ESIR. However, a non-standard type of ampoule was used for the SIR measurement, so the difference may be due to the wall thickness or geometry effects. An attempt to transfer the solution to an SIR-type ampoule was carried out at the BIPM. However, the mass measurement during the transfer failed, making it impossible to interpret the results.

4. Discussion

Table 8 shows the uncertainty budget of the BIPM ESIR system with the minimum, averaged and maximum values encountered among the 13 sets of measurements. The combined uncertainty is largely dominated by the counting statistics with values between 1.2×10^{-4} and 4.2×10^{-4}. The accuracy obtained by the ESIR appears to be slightly better than that of the SIR and is consistent with the need for a transfer instrument for key comparisons in radionuclide metrology. This is made possible by the absence of a calibration component in the budget due to the use of a fixed TDCR model, which does not aim to provide an accurate activity estimate, but to produce a stable reference value. Over two years of monitoring, the consistency of comparison indicators tested using toluene-based LS sources shows no significant long-term fluctuations (see (Coulon et al., 2022b)). However, a long-term drift component may be assessed by statistical analysis of periodic tests and added to the budget to account for these possible variations in the future (Coulon, 2022).

Fig. 4 shows the degrees of equivalence evaluated by the different key comparison indicators of the ESIR. The two self-stabilized

Table 7
Comparison of degrees of equivalence evaluated by the two BIPM transfer instruments, the SIR and the ESIR.

Laboratory	Method	$\delta_{\mathrm{SIR}i}$	$\delta_{\mathrm{ESIR}i}$	Δ_i	Z
ANSTO (1)	LS anticoincidence	0.0208(9)	0.0024(3)	−0.0185(10)	**18.9**
	Ionization chamber	0.0000(9)	−0.0180(3)	−0.0180(10)	**18.6**
ANSTO (2)	LS coincidence	−0.0001(9)	0.0002(4)	0.0004(10)	0.3
	LS anticoincidence	−0.0001(9)	0.0002(4)	0.0004(10)	0.3
	PC coincidence	0.0001(9)	0.0004(4)	0.0002(10)	0.2
BARC	PC coincidence	−0.0035(10)	−0.0196(4)	−0.0160(10)	**15.4**
	SP coincidence	−0.0030(10)	−0.0191(4)	−0.0161(10)	**15.5**
	LS coincidence	0.0010(10)	−0.0152(4)	−0.0162(10)	**15.5**
ENEA-INMRI	Integral counting	0.0048(11)	0.0032(4)	−0.0016(11)	1.4
	TDCR method	0.0071(11)	0.0055(4)	−0.0016(11)	1.4
LNE-LNHB	PC anticoincidence	0.0011(11)	0.0006(4) 0.0023(6)*	−0.0005(12) 0.0011(13)	0.4 0.9
	LS anticoincidence	0.0001(11)	−0.0004(4) 0.0013(6)*	−0.0005(12) 0.0011(13)	0.4 0.9
	TDCR method	0.0011(11)	0.0005(4) 0.0022(6)*	−0.0006(12) 0.0010(13)	0.5 0.8
LNMRI-IRD	LS anticoincidence	−0.0006(9)	−0.0009(5)	−0.0004(10)	0.4
	LS coincidence	−0.0101(9)	−0.0103(5)	−0.0003(10)	0.3
	Peak-sum counting	−0.0006(9)	−0.0009(5)	−0.0003(10)	0.3
	TDCR method	−0.0059(9)	−0.0062(5)	−0.0003(10)	0.3
NIM	PC coincidence	−0.0050(6)	−0.0020(4)	0.0030(7)	**4.1**
	LS coincidence	−0.0040(6)	−0.0030(4)	0.0010(7)	1.4
NIST	LS anticoincidence **	−0.0000(9)	0.0000(4)	0.0000(9)	0.0
NMISA	LS coincidence	0.0008(7)	−0.0008(4)	−0.0017(8)	2.1
NPL	LS coincidence	−0.0006(9)	0.0001(4)	0.0006(10)	0.6
NRC	PC anticoincidence	0.0008(13)	0.0005(4)	−0.0003(14)	0.2
POLATOM	LS coincidence	0.0016(5)	0.0001(5)	−0.0014(7)	2.0
	LS anticoincidence	0.0024(5)	0.0010(5)	−0.0014(7)	2.0
PTB	PC coincidence	0.0010(11)	−0.0043(4)	−0.0053(11)	**4.8**
	LS coincidence	0.0059(11)	0.0006(4)	−0.0053(11)	**4.8**
	C/N method	0.0057(11)	0.0004(4)	−0.0052(11)	**4.7**
	TDCR method	0.0059(11)	0.0006(4)	−0.0053(11)	**4.8**
SMU	TDCR method	−0.0022(9)	−0.0046(5)	−0.0025(10)	2.5
	LS coincidence	0.0006(9)	−0.0018(5)	−0.0024(10)	2.4

*Measurement realized using the μ-TDCR from the LNHB with sources prepared in the same laboratory.
**Used to link the ESIR with the SIR.

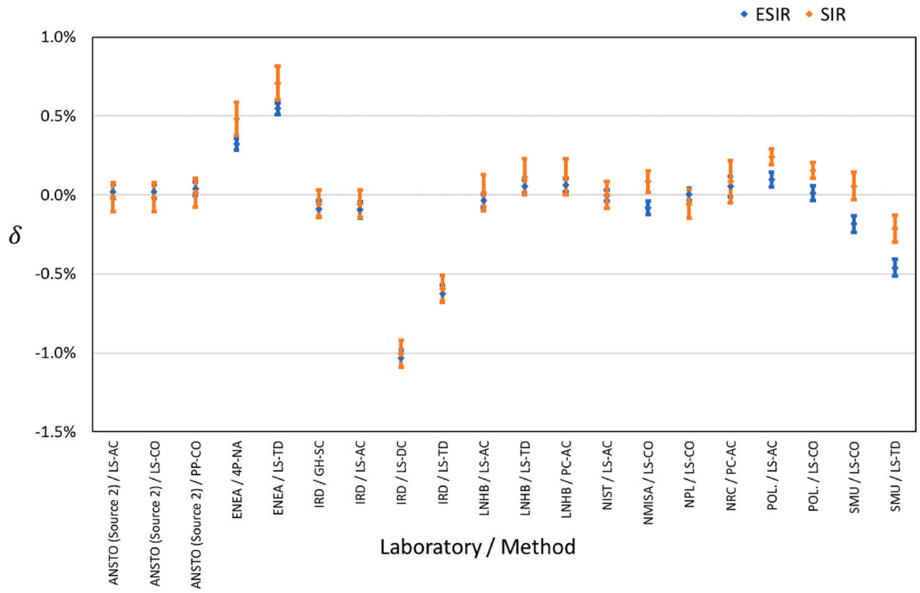

Fig. 2. Relative degrees of equivalence evaluated between SIR and ESIR, in the case where both results are consistent.

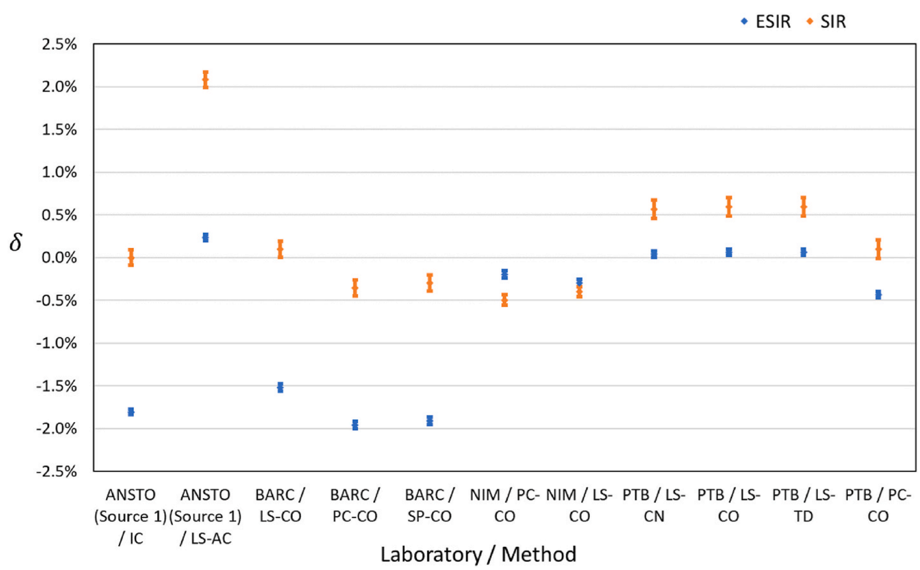

Fig. 3. Relative degrees of equivalence evaluated between SIR and ESIR, in the case where both results are not consistent.

Table 8
Uncertainty budget of the ESIR.

Component	Relative standard uncertainty/100		
	Minimum	Average	Maximum
Background	0.0002	0.0008	0.0013
Counting statistics	0.0116	0.0249	0.0419
Decay correction	0.0016	0.0028	0.0037
Weighing	0.0009	0.0028	0.0050
Combined	**0.0119**	**0.0254**	**0.0421**

comparison indicators, I_1 and I_2, produce superimposed results. This means that during the period of the comparison, the symmetry of the TDCR system was high and remained stable. The raw indicator I_0 significantly differs from the two previous indicators showing that the detection efficiency of the TDCR system had fluctuated during the comparison between 97.7% and 98.1%. This variation could come from various phenomena related to the LS sources chemistry or the electronics chains. These latter variations are efficiently treated by the specific approach of the ESIR.

Table 9 presents the measurements carried out using the several setups to process the TDCR signal. For each configuration, the comparison indicator I_2 is displayed with its standard uncertainty

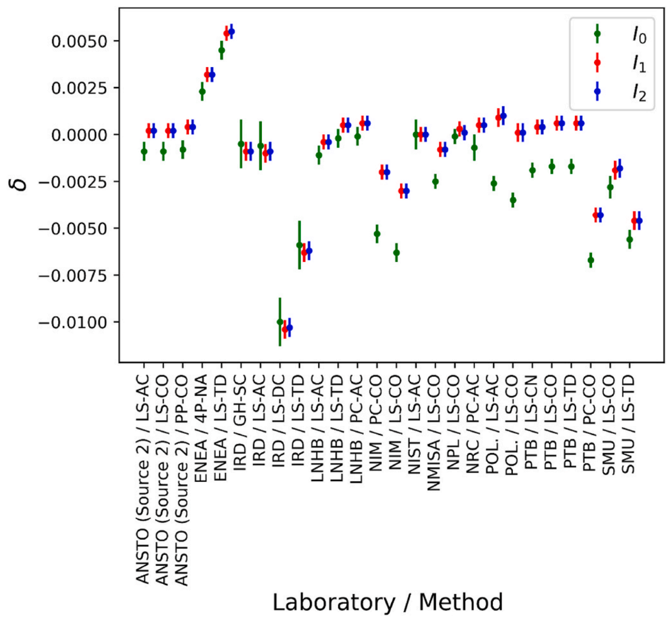

Fig. 4. Degrees of equivalence obtained by the different ESIR comparison indicators (excluding ANSTO source 1 and BARC results).

Table 9
Measurement parameters delivered by the ESIR for different set-up of the TDCR signal processing (case example of the NIST standard solution).

		Extended dead time	
		10 μs	50 μs
Coincidence resolving time	50 ns	I_2 = 86 645(13) Bq g^{-1} t_{dead} = 8.22% $R_{accidental}$ = 0.015%	I_2 = 86 644(11) Bq g^{-1} t_{dead} = 32.82% $R_{accidental}$ = 0.012%
	100 ns	I_2 = 86 658(16) Bq g^{-1} t_{dead} = 8.22% $R_{accidental}$ = 0.030%	I_2 = 86 653(13) Bq g^{-1} t_{dead} = 32.82% $R_{accidental}$ = 0.024%

considering only the counting statistics, and the associated measurement dead time t_{dead} and the accidental coincidence count rate $R_{accidental}$. The comparison indicators agreed to within one standard deviation. The increase of the coincidence resolving time from 50 ns to 100 ns tends to systematically increase by $+2 \times 10^{-4}$ the value of the indicator and doubles the accidental coincidence count rate. However, this slight change has no impact on the degrees of equivalence delivered by the ESIR because the absolute accuracy of the indicator, being used as a normalization factor, does not matter. The increase of the extended dead time from 10 μs to 50 μs changes the measurement dead time from 8.2% to 32.8%. However, this does not impact the indicator value nor the associated standard deviation, proving the robustness of the live-time measurement.

Fig. 5 shows the comparison ratio evaluated at different times for standard solutions from several participating laboratories. It can be observed that the results are reproducible after several months. Nevertheless, as the instability of LS sources was pointed out in the past (Nedjadi et al., 2016), the TDCR measurements will be carried out within two weeks of the LS source preparation.

The standard solution from the LNHB has also been measured by a transportable TDCR system hosted by the LNHB (Sabot et al., 2022). Called here the "LNHB μ-TDCR", it uses the same type of signal processing electronics as the ESIR: the Yantel® nanoTDCR. The raw measurement data from the LNHB μ-TDCR counter was processed in the same way as those coming from the BIPM ESIR system, producing comparison indicators I_{0i}, I_{1i}, I_{2i}. Fig. 6 shows the relative deviations from the two BIPM systems and the transportable LNHB μ-TDCR. The three systems provide comparable results. Such as the BIPM SIRTI (Michotte et al., 2013), this transportable instrument could be envisaged to be linked to the ESIR to provide degrees of equivalence for short-lived radionuclides and laboratories distant from the BIPM headquarters.

All the metadata on this pilot study are available in the following repository: https://github.com/RomainCoulon/CCRI-II-PilotStudy-Co-60.

5. Conclusion

The pilot study demonstrated that the extension of the international reference system for activity, based on the use of a liquid scintillation counter and the TDCR approach, can meet the required accuracy for evaluating a key comparison. Under the real-life conditions of a key

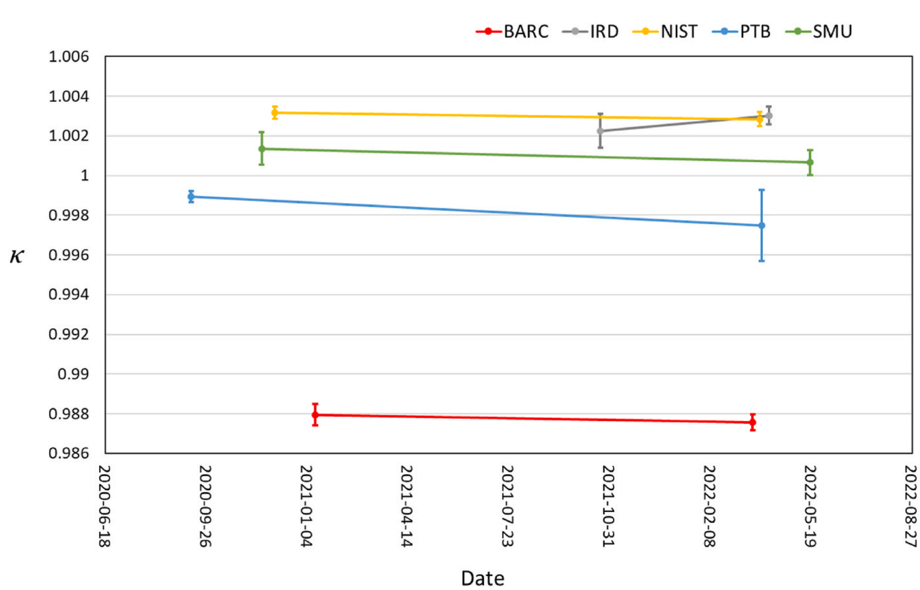

Fig. 5. Repeated measurements of the comparison ratio (error bars are two standard uncertainties).

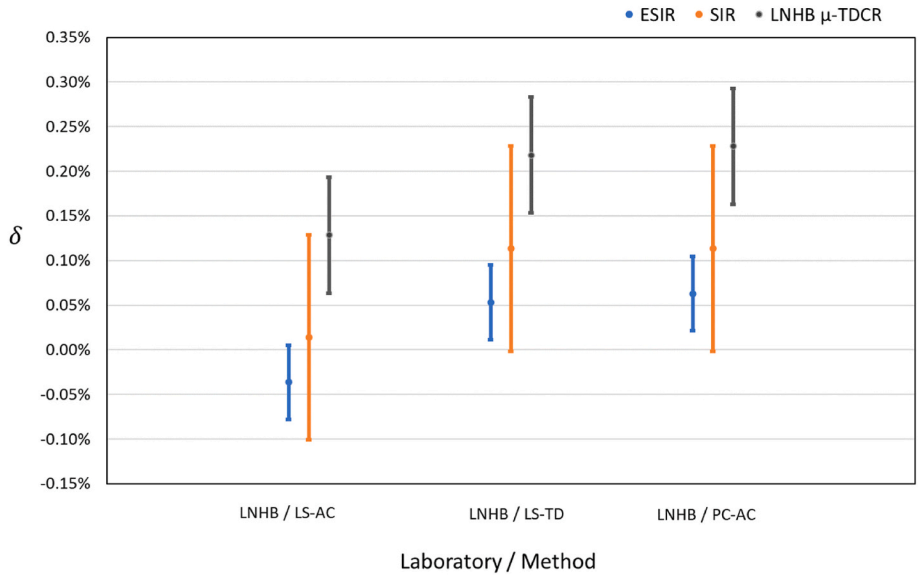

Fig. 6. Relative deviations evaluated by the ESIR, the SIR and the LNHB μ-TDCR of the LNHB submission.

comparison exercise, this new BIPM measurement service provides results in accordance with the original international reference system based on ionization chambers. Taking into account their intrinsic measurement uncertainty, the degrees of equivalence agree between the two BIPM measurement systems and the precision obtained by the new service appears to be on target with a relative standard uncertainty of less than 5×10^{-4}. This is a promising result, validating the approach for radionuclides that decay with sufficient energy release to achieve high detection efficiency (≈98% in the case of ^{60}Co) and for solutions free of radioactive impurities. This result is an important step towards validating the extension of the international reference system for medium- and high-energy beta emitting radionuclides and for alpha emitting radionuclides.

The pilot study also reveals a limitation of the liquid scintillation-based transfer instrument when a low-energy electron emitting impurity is contained in the standard solution. On the other hand, the use of LS methods can also be considered as advantageous, since the use of ionization chambers and PCs alone is not always sufficient to detect impurities – as demonstrated here.

CRediT authorship contribution statement

Romain Coulon: Writing – original draft, Software, Resources, Project administration, Methodology, Conceptualization. **Monica Aguiar Leobino da Silva:** Resources. **Emma Bendall:** Resources. **Denis E. Bergeron:** Writing – review & editing, Resources. **Christophe Bobin:** Writing – review & editing, Resources. **Ivana Bonková:** Resources. **Angus H.H. Bowan:** Resources. **Broda Ryszard:** Writing – review & editing, Resources, Methodology, Conceptualization. **Marco Capogni:** Writing – review & editing, Resources, Methodology. **Mauro Capone:** Resources. **Pierluigi Carconi:** Resources. **Philippe Cassette:** Writing – review & editing, Resources, Methodology, Conceptualization. **T. Cessna Jeffrey:** Writing – review & editing, Resources. **Emily L. Clark:** Resources. **Sean Collins:** Resources. **Sammy Courte:** Resources. **Marek Czudek:** Resources. **Carlos José da Silva:** Writing – review & editing, Resources. **Johnny de Almeida Rangel:** Resources. **Pierino De Felice:** Resources. **Fuyou Fan:** Resources. **Aldo Fazio:** Resources. **Ryan P. Fitzgerald:** Writing – review & editing, Resources. **Carole Fréchou:** Resources. **Raphael Galea:** Resources. **Vincent Gressier:** Supervision, Project administration. **Akira Iwahara:** Resources. **Steven M. Judge:** Supervision, Project administration. **Christine M.B. Keevers:** Resources. **John Keightley:** Resources. **Karsten Kossert:** Writing – review & editing, Resources, Methodology, Conceptualization. **Matej Krivošík:** Resources. **D.B. Kulkarni:** Resources. **Lizbeth Laureano-Perez:** Resources. **Edyta Lech:** Resources. **Anderson Leiras:** Resources. **Juncheng Liang:** Resources. **Paulo Alberto Lima da Cruz:** Resources. **Ronaldo Lins da Silva:** Resources. **Anna Listkowska:** Resources. **Haoran Liu:** Writing – review & editing, Resources, Methodology. **Meiling Liu:** Resources. **Joline Lubbe:** Resources. **Carine Michotte:** Writing – review & editing, Supervision, Resources. **Kimberly Moore:** Resources. **Ole Nähle:** Writing – review & editing, Resources. **Manuel Nonis:** Resources. **Andy Pearce:** Resources. **Leticia Pibida:** Resources. **André L.L. Quadros:** Resources. **Natasha Ramirez:** Resources. **Anuradha Ravindra:** Writing – review & editing, Resources. **Benoit Sabot:** Writing – review & editing, Resources, Methodology. **Paweł Saganowski:** Resources. **V. Sathian:** Resources. **Michael L. Smith:** Resources. **Ritu Sharma:** Resources. **Marcell P. Takács:** Resources. **Milton W. van Rooy:** Writing – review & editing, Resources. **Robert Shearman:** Resources. **Martin J. van Staden:** Resources. **W.M. van Wyngaardt:** Writing – review & editing, Resources. **Zhijie Yang:** Resources. **Melek Zarifi:** Resources. **Ming Zhang:** Resources. **Tomasz Ziemek:** Resources.

Declaration of competing interest

The authors declare that they have no known competing financial interests or personal relationships that could have appeared to influence the work reported in this paper.

Data availability

Data will be made available on request.

Acknowledgement

The authors would like to thank Alain Savary (IRSN) for donating scintillating liquid from his stock to overcome a supply shortage at the BIPM.

References

Bé, M.-M., Chisté, V., Dulieu, C., Browne, E., Chechev, V., Kuzmenko, N., Helmer, R., Nichols, A., Schöfeld, E., Derch, R., 2006. Table of Radionuclides. Monographie BIPM-5 3.

Broda, R., 2003. A review of the triple-to-double coincidence ratio (TDCR) method for standardizing radionuclides. Appl. Radiat. Isot. 58, 585–594. https://doi.org/10.1016/S0969-8043(03)00056-3.

Coulon, R., 2022. Evaluation of the long-term stability of metrology instruments. In: Applied Aspects of Modern Metrology. IntechOpen. https://doi.org/10.5772/intechopen.100511.

Coulon, R., Broda, R., Cassette, P., Courte, S., Dupire, A., Jerome, S., Judge, S., Kossert, K., Liu, H., Michotte, C., Nonis, M., 2022a. The new international reference system for pure α- and pure β-emitting radionuclides and some electron capture decaying radionuclides by liquid scintillation counting. J. Radioanal. Nucl. Chem. https://doi.org/10.1007/s10967-022-08337-7.

Coulon, R., Broda, R., Cassette, P., Courte, S., Dupire, A., Jerome, S., Judge, S., Kossert, K., Liu, H., Michotte, C., Nonis, M., 2022b. The new international reference system for pure α- and pure β-emitting radionuclides and some electron capture decaying radionuclides by liquid scintillation counting. J. Radioanal. Nucl. Chem. 331, 3221–3230. https://doi.org/10.1007/s10967-022-08337-7.

Coulon, R., Broda, R., Cassette, P., Courte, S., Jerome, S., Judge, S., Kossert, K., Liu, H., Michotte, C., Nonis, M., 2020a. The international reference system for pure β-particle emitting radionuclides: an investigation of the reproducibility of the results. Metrologia 57, 035009. https://doi.org/10.1088/1681-7575/ab7e7b.

Coulon, R., Broda, R., Cassette, P., Courte, S., Jerome, S., Judge, S., Kossert, K., Liu, H., Michotte, C., Nonis, M., 2020b. The international reference system for pure β-particle emitting radionuclides: an investigation of the reproducibility of the results. Metrologia 57, 035009. https://doi.org/10.1088/1681-7575/ab7e7b.

Coulon, R., Judge, S., Liu, H., Michotte, C., 2021. The international reference system for pure beta-particle emitting radionuclides: an evaluation of the measurement uncertainties. Metrologia 58, 025007. https://doi.org/10.1088/1681-7575/abe355.

Coulon, R., Michotte, C., Courte, S., Nonis, M., Wyngaardt, W.M. van, Smith, M.L., Bowan, A.H.H., Keevers, C.M.B., Clark, E.L., Zarifi, M., Ravindra, A., Kulkarni, D.B., Sharma, R., Capogni, M., Felice, P. De, Capone, M., Carconi, P., Fazio, A., Bobin, C., Cruz, P.A.L. da, Silva, C.J. da, Silva, R.L. da, Leiras, A., Rangel, J. de A., Silva, M.A.L. da, Iwahara, A., Bergeron, D.E., Cessna, J.T., Fitzgerald, R.P., Laureano-Perez, L., Pibida, L., Rooy, M.W. Van, Lubbe, J., Staden, M.J. van, Shearman, R., Keightley, J., Pearce, A., Ramirez, N., Bendall, E., Collins, S., Ziemek, T., Lech, E., Saganowski, P., Czudek, M., Listkowska, A., Nähle, O., Kossert, K., Takács, M.P., Krivošík, M., Bonková, I., 2023. Update of the BIPM comparison BIPM.RI(II)-K1.Co-60 of activity measurements of the radionuclide ^{60}Co. Metrologia 60, 06010. https://doi.org/10.1088/0026-1394/60/1A/06010.

Dutsov, C., Cassette, P., Sabot, B., Mitev, K., 2020. Evaluation of the accidental coincidence counting rates in TDCR counting. Nucl. Instrum. Methods Phys. Res. 977, 164292 https://doi.org/10.1016/j.nima.2020.164292.

IAEA, 1991. X-Ray and Gamma-Ray Standards for Detector Calibration. IAEA-TECDOC 619.

Jordanov, V., Cassette, P., Dutsov, Ch, Mitev, K., 2020. Development and applications of a miniature TDCR acquisition system for in-situ radionuclide metrology. Nucl. Instrum. Methods Phys. Res. 954, 161202 https://doi.org/10.1016/j.nima.2018.09.037.

Karam, L., Judge, S., Louw, W., 2019. The international measurement system for radionuclide metrology: a strategy for the future. Appl. Radiat. Isot. 154, 108838 https://doi.org/10.1016/j.apradiso.2019.108838.

Kossert, K., Sabot, B., Cassette, P., Coulon, R., Liu, H., 2020. On the photomultiplier-tube asymmetry in TDCR systems. Appl. Radiat. Isot. 163, 109223 https://doi.org/10.1016/j.apradiso.2020.109223.

Lourenço, V., Bobin, C., 2015. Weighing uncertainties in quantitative source preparation for radionuclide metrology. Metrologia 52, S18–S29. https://doi.org/10.1088/0026-1394/52/3/S18.

Michotte, C., Nonis, M., Bobin, C., Altzizoglou, T., Sibbens, G., 2013. The SIRTI: a New Tool Developed at the BIPM for Comparing Activity Measurements of Short-Lived Radionuclides World-wide.

Nedjadi, Y., Duc, P.F., Bochud, F., Bailat, C., 2016. On the stability of ^{3}H and ^{63}Ni Ultima Gold liquid scintillation sources. Appl. Radiat. Isot. 118, 25–31. https://doi.org/10.1016/j.apradiso.2016.08.017.

PTB, 2000. PTB-Ra-16/5, 3-89701-279-0. PTB report.

Ratel, G., 2007. The Système International de Référence and its application in key comparisons. Metrologia 44, 7–16. https://doi.org/10.1088/0026-1394/44/4/S02.

Rytz, A., 1978. International coherence of activity measurements. Environ. Int. 1, 15–18. https://doi.org/10.1016/S0160-4120(78)80071-3.

Sabot, B., Dutsov, C., Cassette, P., Mitev, K., 2022. Performance of portable TDCR systems developed at LNE-LNHB. Nucl. Instrum. Methods Phys. Res. 1034, 166721 https://doi.org/10.1016/j.nima.2022.166721.

van Wyngaardt, F., 2023. Cross-validation of standardisation techniques at ANSTO using Cobalt-60 and subsequent learnings from the presence of non-gamma emitting impurities. Appl. Radiat. Isot. ICRM 2023).